



DRUG DEVELOPMENT AND INDUSTRIAL PHARMACY®

Vol. 29, No. 9, pp. 1035–1044, 2003

RESEARCH PAPER

## Inclusion Complexation of Artemisinin with $\alpha$ -, $\beta$ -, and $\gamma$ -Cyclodextrins

J. W. Wong and K. H. Yuen, Ph.D.\*

School of Pharmaceutical Sciences, University of Science Malaysia,  
Minden, Penang, Malaysia

### ABSTRACT

The present study was conducted to investigate the inclusion complexation of artemisinin (ART) with natural cyclodextrins (CyD), namely  $\alpha$ -,  $\beta$ -, and  $\gamma$ -CyDs with the aim of improving its solubility and dissolution rate. Complex formation in aqueous solution and solid state was studied by solubility analysis, dissolution, and thermal analysis. Solubility diagrams indicated that the complexation of ART and the three CyDs occurred at a molar ratio of 1:1, and showed a remarkable increase in ART solubility. Moreover, the thermodynamic parameters calculated by using the van't Hoff equation revealed that the complexation process was associated with negative enthalpy of formation and occurred spontaneously. The complexation capability of CyDs with ART increased in the order of  $\alpha$ - <  $\gamma$ - <  $\beta$ -CyDs and could be ascribed to the structural compatibility between the molecular size of ART and the diameter of the CyD cavities. Dissolution profiles of the three complexes demonstrated an increased rate and extent of dissolution compared with those of their respective physical mixtures and a commercial preparation. In solid-state analysis, using differential scanning calorimetry, the  $\gamma$ -CyD was capable of complexing the highest percentage of ART, followed by  $\beta$ - and  $\alpha$ -CyDs. The respective estimated percentage of ART complexed by the CyDs were 85%, 40%, and 12%.

**Key Words:** Artemisinin; Cyclodextrins; Complexation.

### INTRODUCTION

Artemisinin (ART) (Fig. 1) and its derivatives are the last few antimalarial drugs that remain effective against multidrug resistant strains of *Plasmodium*

*falciparum* malaria.<sup>[1]</sup> However, ART possesses low aqueous solubility and exhibits a high first-pass metabolism, resulting in poor and variable bioavailability.<sup>[2–4]</sup> This may expose the parasites to sub-therapeutic levels of ART, resulting in incomplete

\*Correspondence: K. H. Yuen, Ph.D., School of Pharmaceutical Sciences, University of Science Malaysia, 11800 Minden, Penang, Malaysia; Fax: 604-6596517; E-mail: khyuen@usm.my.

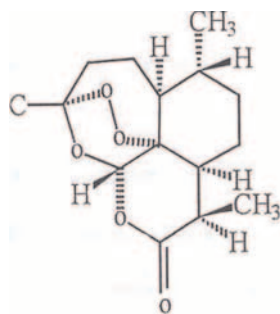


Figure 1. The chemical structure of artemisinin.

parasite elimination and, hence, recrudescence.<sup>[3]</sup> Moreover, absorption of ART has been observed to be limited to the upper part of the gastrointestinal tract with negligible or no absorption occurring in the large intestine.<sup>[5,6]</sup> However, ART has good intestinal permeability and readily crosses the intestinal monolayers easily via passive diffusion.<sup>[7]</sup> Thus, improving its aqueous solubility may help to increase its bioavailability.

Cyclodextrins (CyD), with their unique architecture, are rapidly gaining recognition as useful pharmaceutical excipients for increasing the solubility/dissolution and, hence, the bioavailability of poorly water-soluble drugs.<sup>[8,9]</sup> However, the capability of CyDs to form inclusion complexes is not extended to every drug that suffers from such a limitation. This complexation ability of CyDs is governed by the geometrical fitness of the guest molecule inside the CyD cavities, as well as the charge and polarity criteria of the guest molecule.<sup>[10,11]</sup>

The present study was conducted to investigate the inclusion complexation of ART with natural CyDs, namely  $\alpha$ -,  $\beta$ -, and  $\gamma$ -CyDs with the aim of improving its solubility and dissolution.

## MATERIALS AND METHODS

### Materials

$\alpha$ -,  $\beta$ -, and  $\gamma$ -CyD were obtained from Cerestar (Indianapolis, IN). Artemisinin was obtained from Kunming Pharmaceutical Corporation (Kunming, China). All other chemicals and reagents used were either analytical or high-performance liquid chromatography (HPLC) grade. A commercially available product, Artemisinin 250<sup>®</sup> capsule (Mekophar, Vietnam), containing the normal form of the drug with batch number VNA 1350-98 and manufactured in May 1998, was used as a reference preparation.

### Phase Solubility Studies

The complexing capacity of  $\alpha$ -,  $\beta$ -, and  $\gamma$ -CyD with ART in aqueous solution was quantified by using the solubility method<sup>[12]</sup> at 24°C, 37°C, and 52°C. Excess amounts of ART were added to increasing concentrations of  $\alpha$ -,  $\beta$ -, and  $\gamma$ -CyD solutions in Erlenmeyer flasks. The concentrations used were 0 mM, 20 mM, 40 mM, 60 mM, 80 mM, and 100 mM for  $\alpha$ -CyD; 0 mM, 2 mM, 4 mM, 8 mM, 12 mM, and 14 mM for  $\beta$ -CyD; and 0 mM, 25 mM, 50 mM, 100 mM, 125 mM, and 175 mM for  $\gamma$ -CyD. The flasks were then shaken continuously in a thermostatically controlled water bath for 72 hr until equilibrium was achieved, as demonstrated by a constant ART concentration at 72 hr and 96 hr. After equilibrium was attained, a 5 mL sample of each solution was filtered through a 0.2- $\mu$ m nylon membrane and diluted with water before analysis. The stability constants ( $K_{s1:1}$ ) of complexation at the three different temperatures for each CyD were then calculated from the linear section of the phase solubility diagrams, assuming that a 1:1 stoichiometric ratio complex was formed at the initial step. The stability constant  $K_{s1:1}$  was calculated by using the following relationship:

$$K_{s1:1} = \frac{\text{slope}}{S_0(1 - \text{slope})}$$

where  $S_0$  is the intrinsic solubility of ART in the absence of CyD, and the slope refers to the gradient of the plot of ART solubility (mM) vs. CyD concentration (mM).

Furthermore, the enthalpy change ( $\Delta H$ ), entropy change ( $\Delta S$ ), and free energy change ( $\Delta G$ ) for the formation of  $\alpha$ -,  $\beta$ -, and  $\gamma$ -CyD-ART complexes were investigated by using the temperature-dependent characteristic of the stability constant based on the van't Hoff equation<sup>[13,14]</sup> as shown below:

$$\ln K_{s1:1} = -\frac{\Delta H}{RT}$$

in which  $K_{s1:1}$  is as defined above,  $T$ , the absolute temperature (Kelvin); and  $R$ , the gas constant (8.314 J/mol/K). The  $\Delta H$  (enthalpy change) was calculated from the slope of the plot of  $\ln K_{s1:1}$  vs.  $1/T$  after least square linear regression analysis. This was followed by calculating the  $\Delta G$  and  $\Delta S$  for each temperature by using the following equations.<sup>[15]</sup>

$$\Delta G = -RT \ln K_{s1:1}$$

$$\Delta S = \frac{\Delta H - \Delta G}{T}$$

### Preparation of CyD-ART Complexes

The  $\alpha$ -,  $\beta$ -, and  $\gamma$ -CyD complexes were prepared by using a slurry method at a molar ratio of 1:1 (CyDs:ART). The batch size for each preparation was maintained between 20–30 g. The CyDs were individually mixed with water until a homogenous suspension was obtained. The ART, which previously had been ground and passed through a sieve size of 300  $\mu$ , was then added into the suspensions. The mixtures were stirred for 24 hr at 26–28°C before being dried under an extraction fan. The resulting complexes were ground in a glass mortar and sieved through 300  $\mu$  mesh. The temperature, amount of water, mixing time, and drying conditions used were kept constant during the preparation of each new batch. In addition, pure ART and CyDs also were individually subjected to the same manner of preparation, which were then used to prepare physical mixtures at molar ratio equal to that of the complexes (1:1) by gently mixing with a spatula. The uniformity of the physical mixtures was determined by using thermal analysis, and they were deemed homogeneous if the thermograms obtained from three separate samples taken from the same mixture were superimposable and the area under the ART endotherm (heat of fusion of ART) did not deviate by more than 10% for the three samples.

### Dissolution Studies

The in vitro dissolution of the  $\alpha$ -,  $\beta$ -, and  $\gamma$ -CyD complexes, their respective physical mixtures, as well as the commercial product was determined by using the paddle method (Pharma Test, Hainburg, Germany) in 900 mL of distilled water, under nonsink conditions. The paddle rotation speed was set at 100 rpm. The temperature was maintained at  $25 \pm 0.5^\circ\text{C}$  because, at a higher temperature, ART would recrystallize out of the collected samples on exposure to room temperature. Preparations containing an equivalent amount of 250 mg of ART were used for the dissolution. However, in the experiments comparing the dissolution profiles of the  $\alpha$ -,  $\beta$ -, and  $\gamma$ -CyD complexes with their corresponding physical mixtures, the weights of the preparations used contained an equivalent of 150 mg of ART. Samples of 5-mL volume were collected at 15, 30, 45 min and at 1, 1.5, 2, 3, 4, 6, and 8 hr by using an automated fraction collector (SDX Fractional Collector, Penang, Malaysia).

### Analysis of ART Concentration

The ART concentration for the above phase solubility and dissolution studies was analyzed by using a HPLC method.<sup>[16]</sup> The system comprised a Jasco PU-980 pump (Tokyo, Japan), an electrochemical detector (Antec-Leyden, Leiden, The Netherlands), a Rheodyne 7725i injector (Rheodyne, CA, US) fitted with a 20  $\mu\text{L}$  sample loop and a Corsil CN-RP column (Bioscience, Kuala Lumpur, Malaysia). The flow cell was equipped with a glassy carbon working electrode and an Ag/AgCl reference electrode saturated with lithium chloride. The mobile phase consisted of 0.1 M ammonium acetate buffer adjusted to pH 5.5 with glacial acetic acid and acetonitrile (75:25; v/v) with the flow rate set at 1.4 mL/min. Deoxygenation of the mobile phase was achieved by heating at 50°C for 2 hr and then maintained at 30°C while purging with Argon. The detector was operated in reductive mode at an applied potential of  $-1.0\text{ V}$ , a sensitivity of 10 nA f.s., and the signal was filtered at 0.1 sec.

### Differential Scanning Calorimetry Studies

Differential scanning calorimetry (DSC) studies were performed on the individual components (before and after slurring), the complexes, and, the physical mixtures by using a TA Instruments model 2010 differential scanning calorimeter (Newcastle, DE, US) equipped with a Universal Analysis software. Samples between 2.5–5.0 mg were placed in hermetic aluminium pans pierced with a pinhole and scanned from 25°C to 200°C at 10°C/min. Nitrogen was used as the purge gas, with the flow rate set at 50 mL/min.

An attempt also was made to estimate the percentage of ART complexed with each of the CyDs by comparing the thermograms of the complexes with their respective physical mixtures at equal weights. The area under the peak melting temperature of ART ( $\Delta H_{\text{art}}$ ) is directly proportional to the amount of ART. Thus, the ART peak observed in the thermograms of the complexes was representative of the uncomplexed drug, and the percentage of ART complexed was then calculated by using the following relationship:

$$\frac{\Delta H_{\text{art}} \text{ of the physical mixtures} - \Delta H_{\text{art}} \text{ of the CyD complexes}}{\Delta H_{\text{art}} \text{ of the physical mixtures}} \times 100\%$$

An evaluation of the DSC method used to quantify the percentage of complexation also was carried out to determine the linearity, within and between day accuracy and precision by using the following known weights of ART, namely, 0.5, 1.0, 2.0, 3.0, 4.0, and 5.0 mg. The accuracy was expressed as the percentage of the measured weight over that of the actual value, whereas the precision was denoted by using the coefficient of variation ( $n=3$ ).

## RESULTS AND DISCUSSION

### Phase Solubility and Thermodynamic Studies

Figures 2, 3, and 4 show the phase solubility diagrams for  $\alpha$ -,  $\beta$ -, and  $\gamma$ -CyD-ART systems in water, respectively. In all systems, the linear solubility curves could be classified as type A<sub>L</sub>, indicating the systems were first order in nature.<sup>[12]</sup> The linear relationship also implied that dilution of a solution of a ART-CyD complex during administration into the body would not cause precipitation of a ART regardless of the extent of dilution. Moreover, it also indicated that the aqueous solubility of ART per mM of CyDs used was greatly enhanced in the order of  $\beta > \gamma > \alpha$  for the three temperatures studied, as reflected in the values of the slope of the three

phase solubility diagrams and the stability constants shown in Table 1. There was an almost 16.9-fold difference between the stability constant value of  $\beta$ -CyD and that of  $\alpha$ -CyD (at 24°C), and a 3.4-fold difference when compared with that of  $\gamma$ -CyD.

The stability constant value can be referred to as the strength or magnitude of complexation of ART to the CyD cavity.<sup>[17]</sup> Hence,  $\beta$ -CyD has the strongest complex-forming ability with ART, while that of the  $\alpha$ -CyD can be considered negligible. As for  $\gamma$ -CyD, the values were intermediate between those of  $\alpha$ - and  $\beta$ -CyDs. The high stability constant values of  $\beta$ -CyD also reflect favorable positioning or fitness of the drug inside the cavity of the CyD molecules, implying a better spatial relationship between ART and  $\beta$ -CyD.<sup>[18]</sup> In the case of  $\gamma$ -CyD, its cavity may be too large, enabling the ART molecule to move more freely in and out of the cavity, resulting in a weaker complex being formed, while that of  $\alpha$ -CyD may be too small to allow penetration of the ART molecule.

The values of the thermodynamic parameters for the three systems are shown in Table 1. In all cases, the complexation process was associated with negative enthalpy of formation, indicating that complex formation was an exothermic process. The complexation of  $\beta$ -CyD with ART was enthalpically driven, characterized by a large enthalpy change and a very small entropy change. The former could be due

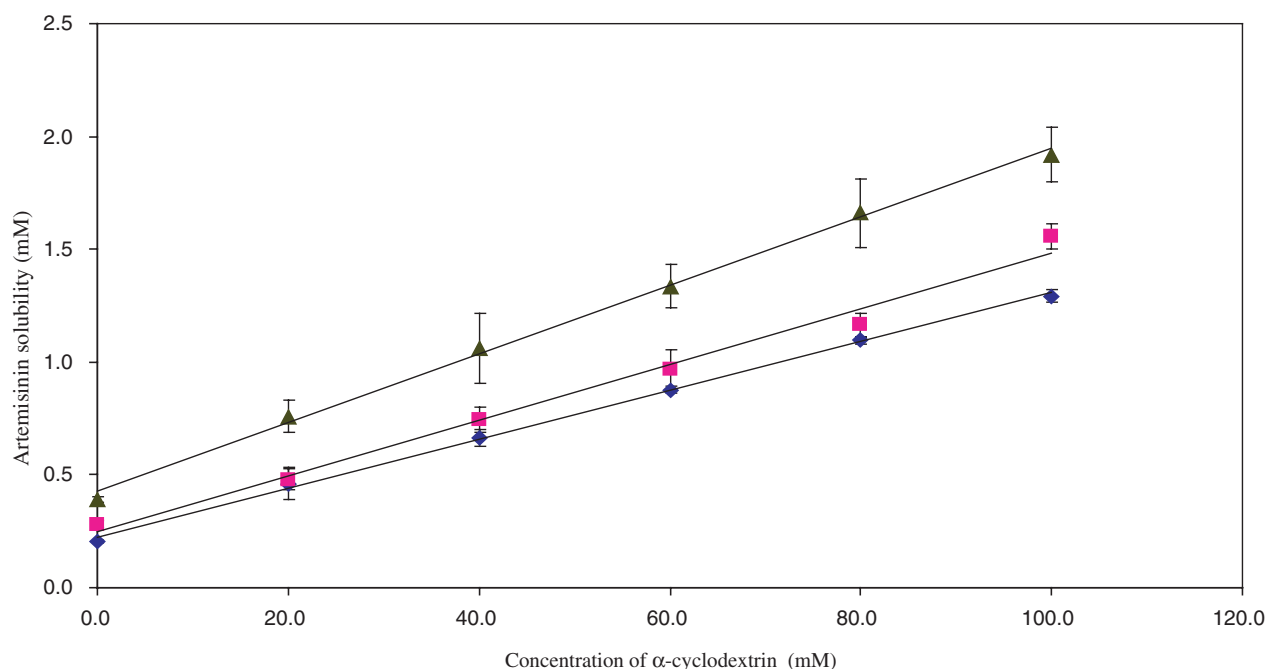


Figure 2. Phase solubility diagram of  $\alpha$ -CyD-ART system at 25°C, 37°C, and 52°C. ◆ = 24°C, ■ = 37°C, ▲ = 52°C.

## Inclusion Complexation of Artemisinin

1039

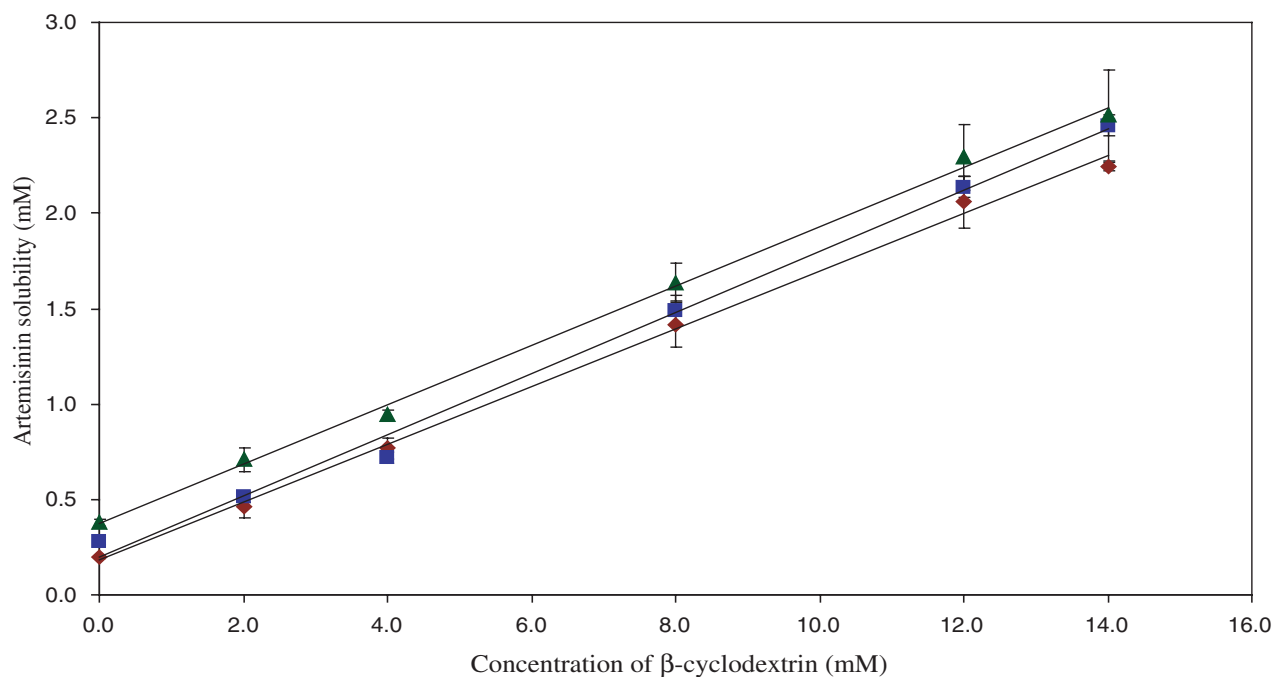


Figure 3. Phase solubility diagram of  $\beta$ -CyD-ART system at 25°C, 37°C, and 52°C.  $\blacklozenge$  = 24°C,  $\blacksquare$  = 37°C,  $\blacktriangle$  = 52°C.

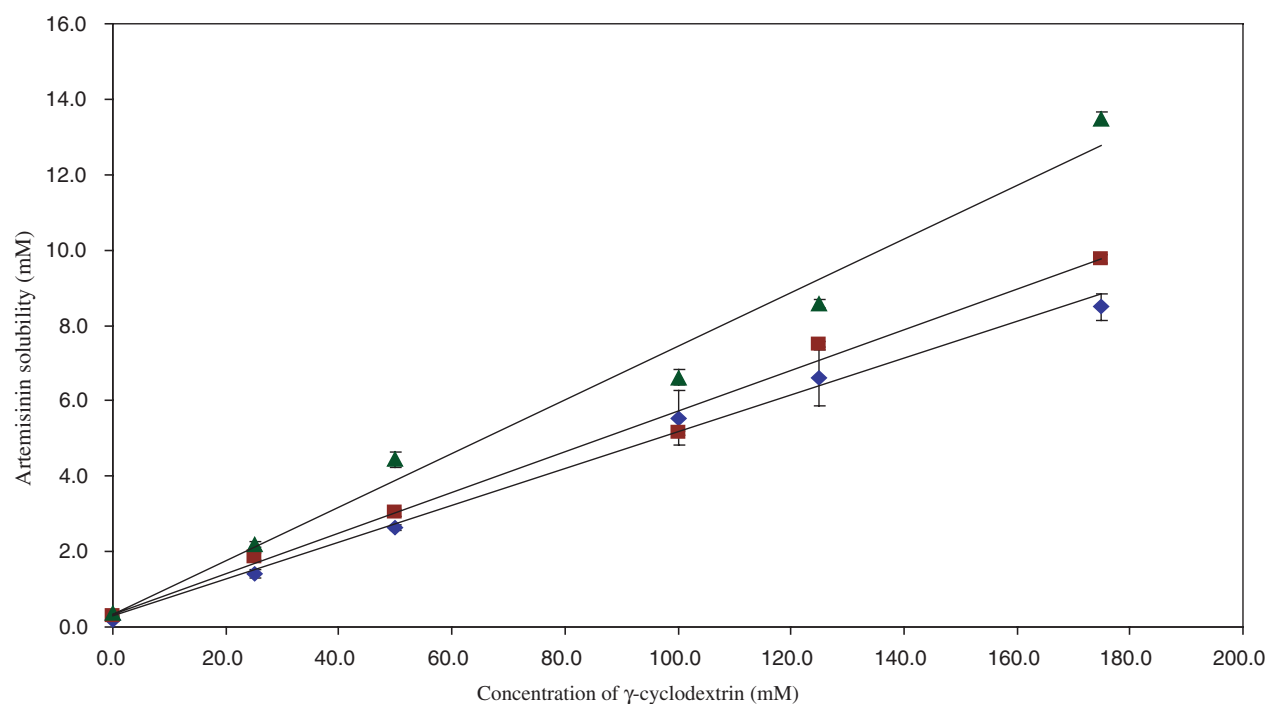


Figure 4. Phase solubility diagram of  $\gamma$ -CyD-ART system at 25°C, 37°C, and 52°C.  $\blacklozenge$  = 24°C,  $\blacksquare$  = 37°C,  $\blacktriangle$  = 52°C.

to the snug fit and deep penetration of ART inside the  $\beta$ -CyD cavity resulting in more enthalpy-rich water molecules being displaced. Moreover, the smaller distance between ART and  $\beta$ -CyD cavity

wall could lead to a stronger exothermic van der Waals–London dispersion forces, thus contributing toward the enthalpy of complexation. The favorable fit between ART and  $\beta$ -CyD also could contribute to



**Table 1.** Stability constants ( $K_{s1:1}$ ) and thermodynamic parameter values for  $\alpha$ -,  $\beta$ -, and  $\gamma$ -CyD complexes at 24°C, 37°C, and 52°C, as well as the correlation coefficients of the van't Hoff plots.

Temperature (°C)	$\alpha$ -Cyclodextrin complex				$\beta$ -Cyclodextrin complex				$\gamma$ -Cyclodextrin complex			
	$\Delta H$ (kJ/mol)	$\Delta G$ (kJ/mol)	$\Delta S$ (J/mol. K)	$K_{s1:1}$ (M <sup>-1</sup> ) (SD)	$\Delta H$ (kJ/mol)	$\Delta G$ (kJ/mol)	$\Delta S$ (J/mol. K)	$K_{s1:1}$ (M <sup>-1</sup> ) (SD)	$\Delta H$ (kJ/mol)	$\Delta G$ (kJ/mol)	$\Delta S$ (J/mol. K)	$K_{s1:1}$ (M <sup>-1</sup> ) (SD)
24	-8.64	-9.82	3.96	53.3 (1.2)	-17.54	-16.78	-2.54	894.3 (42.6)	-7.47	-13.75	21.14	262.1 (16.1)
37	-8.64	-9.79	3.71	44.6 (2.1)	-17.54	-16.81	-2.33	680.9 (18.0)	-7.47	-13.70	20.10	203.6 (11.1)
52	-8.64	-9.92	3.95	39.4 (2.2)	-17.54	-16.71	-2.53	485.3 (35.7)	-7.47	-14.34	21.13	201.6 (9.3)
* $r^2$			0.998				0.997				0.992	

\* $r^2$  = correlation coefficient of the van't Hoff plot.

the small negative entropy change observed. A tight packing could cause the movement of  $\alpha$ -1,4 glycosidic linkages in the  $\beta$ -CyD molecules to be restricted. While these factors might have contributed to a negative entropy change, their effects were masked to some extent by the breakdown of highly structured water molecules inside the  $\beta$ -CyD cavity. As a result, only a small negative entropy change was observed.<sup>[19]</sup>

In comparison, complexation between ART to  $\gamma$ -CyD showed a relatively small exothermic  $\Delta H$ . The water molecules that resided inside the  $\gamma$ -CyD were not as enthalpy rich as  $\beta$ -CyD, due to its smaller cavity size, but more similar to the bulk water. Thus, expulsion of these water molecules from the CyD cavity during complexation did not contribute much to the enthalpy change, and, therefore, only a small negative change was observed.<sup>[20]</sup> Moreover, the distance between the included ART and the cavity wall of  $\gamma$ -CyD tended to be larger, resulting in weaker exothermic van der Waals forces. On the other hand, the comparatively larger positive entropy value might be attributed mainly to the loose fit of ART inside the cavity, thus enabling the ART molecules to move in and out of the CyD cavity. This, in turn, caused structural breakdown of water molecules around the ART molecules. A larger number of water molecules also would be released, resulting in an increase in the randomness of the system.

In comparison, the complexation of  $\alpha$ -CyD-ART displayed the smallest  $\Delta H$  and a slightly favorable  $\Delta S$ . This may be due to the comparatively small cavity of  $\alpha$ -CyD for accommodating the ART molecule, whereby the ART molecule could not penetrate deeply but merely sat on top of the cavity. This shallow penetration would provide a smaller area of contact between ART and  $\alpha$ -CyD, and, therefore, the binding forces were relatively weak.

Similar observations were made with the  $\Delta G$ , which is related to the match between the molecular size of ART and the diameter of the CyD cavities<sup>[21]</sup> The values of  $-\Delta G$  increased in the order of  $\alpha < \gamma < \beta$ . A clear relationship was seen between the  $\Delta G$  and the structural compatibility of the CyD cavity. Moreover, the thermodynamic data was consistent with the values of the stability constants obtained, in terms of the ability of CyD to complex with ART.

### Dissolution Studies

The dissolution profiles of the  $\alpha$ -,  $\beta$ -, and  $\gamma$ -CyD complexes, together with that of the commercial preparation, are shown in Fig. 5. It is apparent that all the preparations reached a saturated concentration within 1.5 hr, with the  $\alpha$ - and  $\gamma$ -CyD complexes displaying faster rates than the other two preparations. In terms of the extent of dissolution, the saturation solubility achieved was in the order of  $\beta > \gamma > \alpha$ -CyD complexes > reference preparation. The higher rate and extent of dissolution of the complexes may be attributed to the hydrophilic effect of CyDs, which reduced both the hydrophobicity of ART as well as the interfacial tension between ART and the dissolution medium. Moreover, the solubility of ART was increased by the CyDs. In addition, complexation is capable of reducing the particle size and crystallinity of ART to an extent not achievable by normal grinding and, thus, contributing further to the increased rate of dissolution. It also is evident that the concentration of ART dissolved from both the  $\alpha$ -CyD and  $\gamma$ -CyD complexes decrease gradually after reaching the saturation solubility but not with the  $\beta$ -CyD complex. The phenomenon could be ascribed to the recrystallization of ART from the dissolution

## Inclusion Complexation of Artemisinin

1041

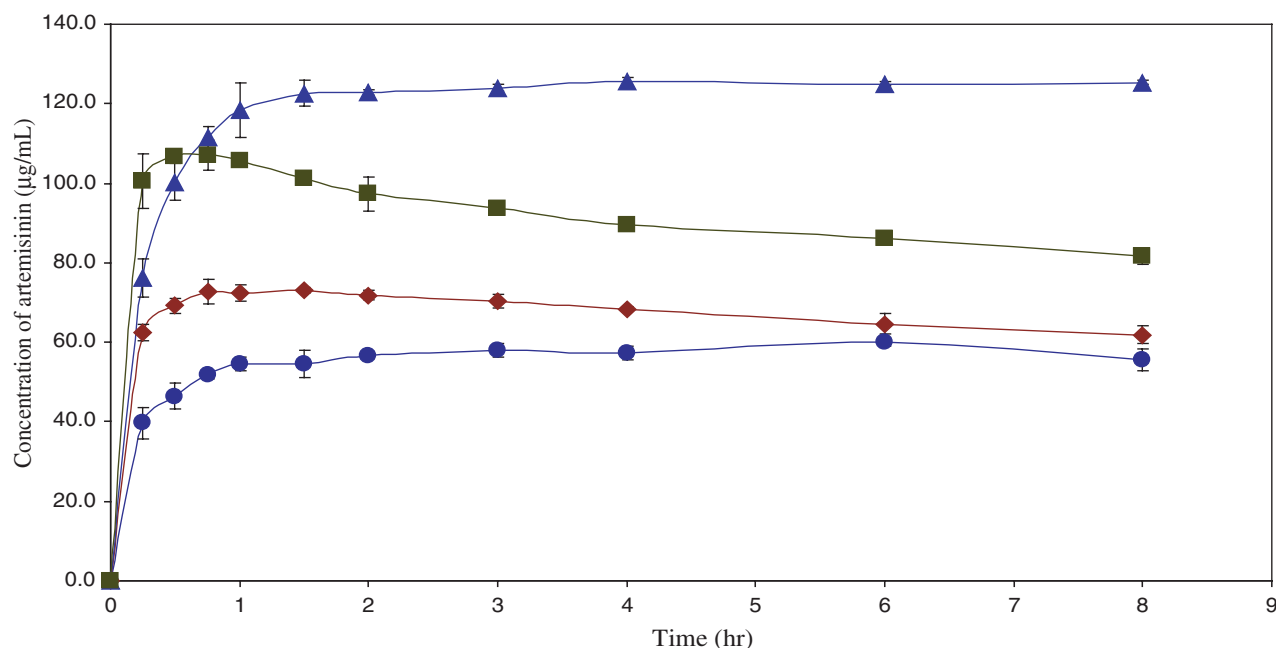


**Figure 5.** Mean dissolution profiles of commercial preparation and CyD-ART complexes (250 mg of artemisinin). Mean  $\pm$  SD.  $N=4$ .  $\blacktriangle$  =  $\beta$ -CyD complex,  $\blacksquare$  =  $\gamma$ -CyD complex,  $\blacklozenge$  =  $\alpha$ -CyD complex,  $\bullet$  = commercial preparation.

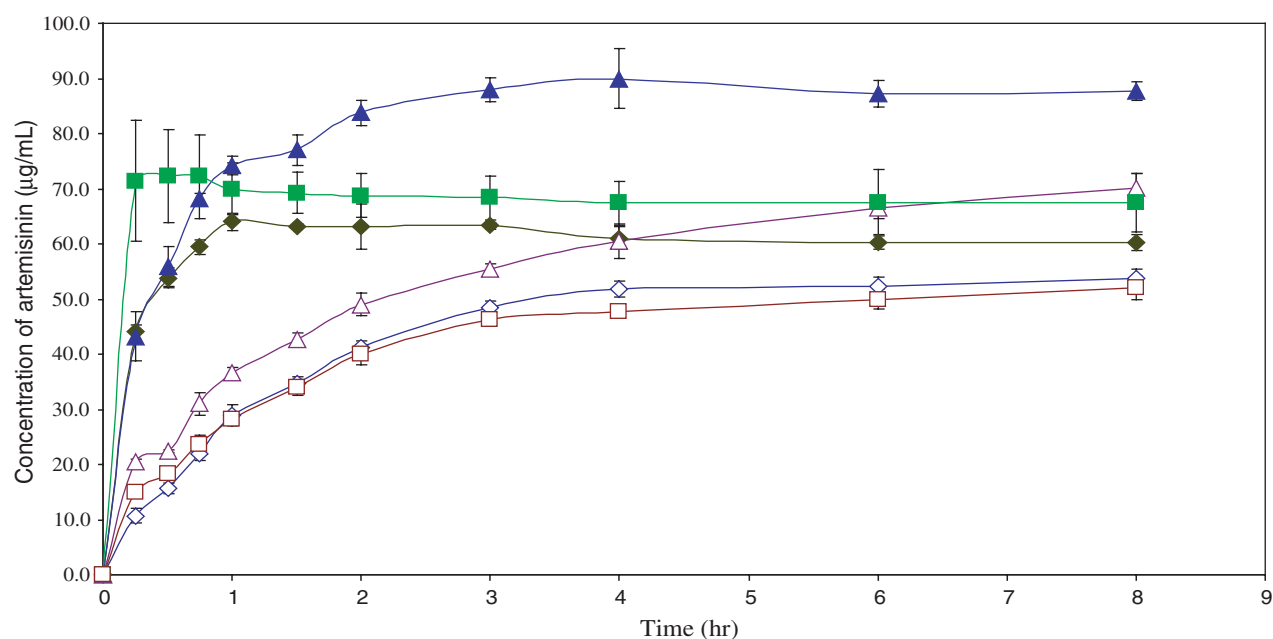


**Figure 6.** Mean dissolution profiles of CyD-ART complexes and their respective physical mixtures (150 mg of artemisinin). Mean  $\pm$  SD.  $N=4$ .  $\blacktriangle$  =  $\beta$ -CyD complex,  $\blacksquare$  =  $\gamma$ -CyD complex,  $\blacklozenge$  =  $\alpha$ -CyD complex,  $\triangle$  = physical mixture of  $\beta$ -CyD and ART,  $\diamond$  = physical mixture of  $\alpha$ -CyD and ART,  $\square$  = physical mixture of  $\gamma$ -CyD and ART.

medium, thus suggesting that the  $\beta$ -CyD is more capable of stabilizing the supersaturated solution, possibly due to the better fit of the ART molecule in the  $\beta$ -CyD cavity.

Figure 6 shows the dissolution profiles of the  $\alpha$ -,  $\beta$ - and  $\gamma$ -CyD complexes and their respective physical mixtures. It can be observed that all complexes achieved both a higher rate and extent of dissolution

compared with their respective physical mixtures. Moreover, it also is interesting to note that the three physical mixtures displayed different extents of dissolution in a similar rank order to that observed with the complexes. This can be explained on the basis of the solubility of ART in the aqueous CyD solutions. It can be assumed that in the early stages of the dissolution process, transient inclusion complexation by the CyDs was occurring on the hydrodynamic layer surrounding the ART particles.  $\beta$ -CyD complexes have the highest stability constant and would, therefore, induce the highest amount of ART to be dissolved, compared with  $\alpha$ - and  $\gamma$ -CyDs.

### DSC Studies

The validation results showed that the method for the quantitative analysis by using DSC displayed satisfactory accuracy and precision. For both within-day and between-day, the accuracy values were all less  $\pm 5.5\%$ , while, for the precision, all the coefficient

of variation values were less than 10.2% at the weights determined. Moreover, the  $\Delta H_{\text{art}}$  was linear over the range of 0.5 mg to 6.0 mg of ART, with a correlation coefficient of 0.9998. The limit of quantification was 0.5 mg, the lowest weight that can be weighed accurately by using a microbalance (Mettler M3 Microbalance, Schwerzenbach, Switzerland).

The DSC responses of pure ART,  $\alpha$ -,  $\beta$ -,  $\gamma$ -CyDs, and their respective samples that were subjected to slurry processing are essentially similar, indicating that there was no change in their physical characteristics. The ART showed a sharp melting endotherm at a temperature of  $153.7 \pm 0.5^\circ\text{C}$ , being similar to that reported by Jinadasa<sup>[5]</sup> for the orthorhombic polymorphic form of the drug. Moreover, the thermogram of the reference preparation also has a melting point of  $153.7 \pm 0.1^\circ\text{C}$ , being similar to that of the ART used in the present study, and, thus, both could be of the same polymorphic form.

The thermograms of the  $\alpha$ -,  $\beta$ -, and  $\gamma$ -CyD complexes and their respective physical mixtures are

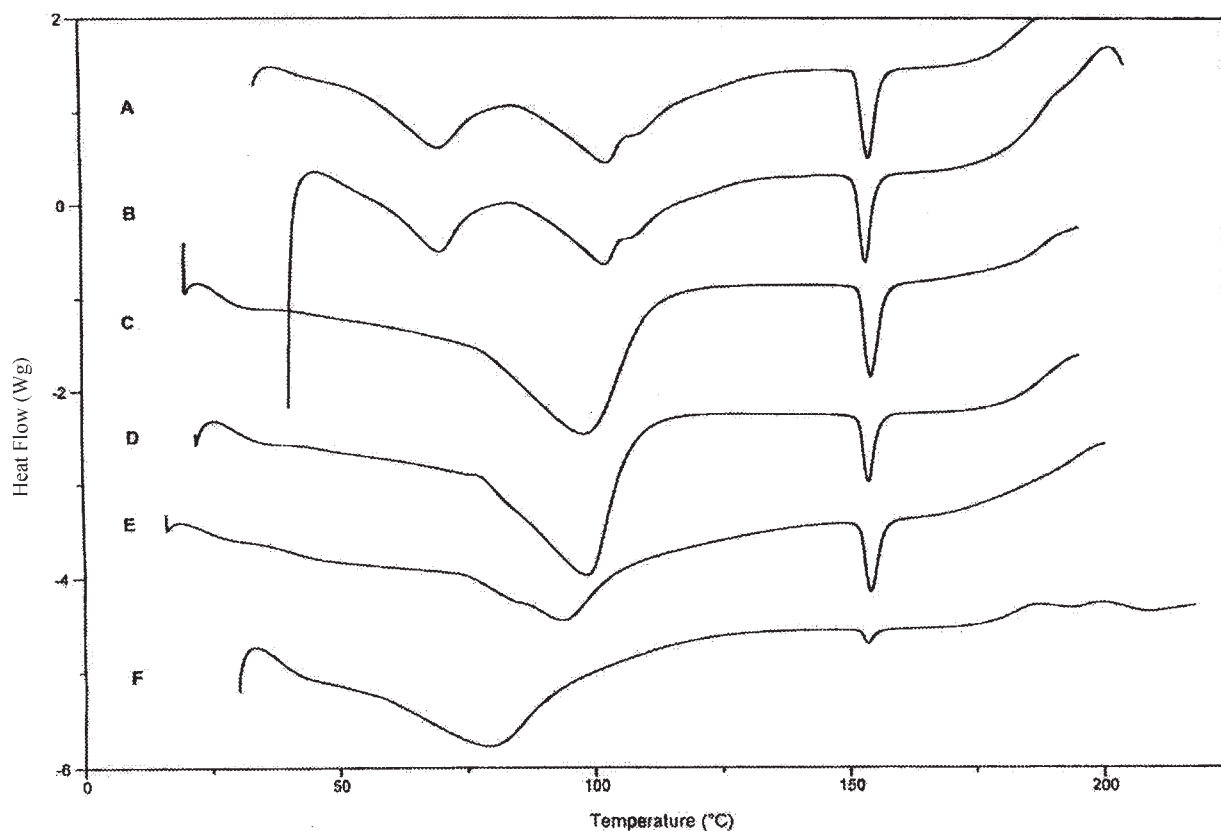


**Figure 7.** Thermograms of  $\alpha$ -,  $\beta$ -, and  $\gamma$ -CyD complexes and their respective physical mixtures. A = physical mixture of  $\alpha$ -CyD and ART, B =  $\alpha$ -CyD complex, C = physical mixture of  $\beta$ -CyD and ART, D =  $\beta$ -CyD complex, E = physical mixture of  $\gamma$ -CyD and ART, F =  $\gamma$ -CyD complex.



## Inclusion Complexation of Artemisinin

1043

shown in Fig. 7. The thermograms of the three physical mixtures were essentially a superimposition of the DSC responses of the individual components of ART and CyDs. No change in the melting temperature of ART was recorded. This was similarly observed with the CyD complexes but was accompanied by a reduction in the  $\Delta H_{\text{art}}$ , suggesting that complexation occurred between the CyDs and ART. However, it is apparent that the degree of complexation was different among the three CyDs used, as evidenced by the differences in reduction of  $\Delta H_{\text{art}}$ . The  $\gamma$ -CyD complex showed the largest reduction in the  $\Delta H_{\text{art}}$ , of approximately 85%, suggesting that this percentage of ART was being complexed. For  $\beta$ - and  $\alpha$ -CyD complexes, the values were about 40% and 12%, respectively, thus inferring that the complexation ability of CyDs for ART in solid state decreased from  $\gamma > \beta > \alpha$ -CyDs. It is interesting to note that the degree of ART complexation with the three CyDs estimated from the DSC studies did not follow the same order as their complexation ability determined from the phase solubility studies. Nevertheless, the  $\beta$ -CyD complexes still showed an almost comparable rate but higher extent of dissolution than that of the  $\gamma$ -CyD complex. Thus, it appeared that the lower degree of complexation of ART with  $\beta$ -CyD with respect to that of  $\gamma$ -CyD did not adversely affect its dissolution properties. However, it should be noted that the reduction in  $\Delta H_{\text{art}}$  of all the three complexes studied also could, in part, be ascribed to the presence of an amorphous fraction of the drug.

## CONCLUSION

From the above analysis, it can be inferred that the  $\alpha$ -,  $\beta$ -, and  $\gamma$ -CyDs were capable of interacting to form complexes with ART. The complexes showed higher saturation solubility with an increased rate of dissolution as compared with the commercial preparation as well as physical mixtures of the drug and CyDs. The degree of complexation in solution increased in the order of  $\beta > \gamma > \alpha$ -CyDs, while in the solid state, it was  $\gamma > \beta > \alpha$ -CyDs.

## REFERENCES

1. World Health Organization. The use of artemisinin and its derivatives as anti-malarial drugs. Reports of a joint CTD/DMP/TDR informal consultation; World Health Organization, Geneva, 1998; mimeographed document WHO/MAL/98.1086.
2. Luo, X.D.; Shen, C.C. The chemistry, pharmacology and clinical applications of Qinghaosu (artemisinin) and its derivatives. *Med. Res. Rev.* **1987**, *7*, 29–52.
3. Titulaer, H.A.C.; Zuidema, J.; Kager, P.A.; Wetsteyn, J.C.F.M.; Lugt, C.H.B.; Merkus, F.W.H.M. The pharmacokinetics of artemisinin after oral, intramuscular and rectal administration to volunteers. *J. Pharm. Pharmacol.* **1990**, *42*, 810–813.
4. Svensson, U.S.H.; Sandström, R.; Carlborg, O.; Lennernäs, H.; Ashton, M. High in situ rat intestinal permeability of artemisinin unaffected by multiple dosing and with no evidence of *P*-glycoprotein involvement. *Drug Metab. Disp.* **1999**, *27* (2), 227–232.
5. Jinadasa, S. Analysis and production of artemisinin, and antimalarial from *Artemisia annua* L, Ph.D. Thesis, University of Science: Malaysia, 1996.
6. Wong, J.W.; Yuen, K.H. Improved oral bioavailability of artemisinin through inclusion complexation with  $\beta$ - and  $\gamma$ -cyclodextrins. *Int. J. Pharm.* **2001**, *227*, 177–185.
7. Augustijns, P.; D'Hulst, A.; Daele, J.V.; Kinget, R. Transport of artemisinin and sodium artesunate in caco-2 intestinal epithelial cells. *J. Pharm. Sci.* **1996**, *85* (6), 577–579.
8. Uekama, K.; Horiuchi, Y.; Kikuchi, M.; Hirayama, F.; Ijitsu, T.; Ueno, M. Enhanced dissolution and oral bioavailability of  $\alpha$ -tocopherol esters by dimethyl- $\beta$ -cyclodextrin complexation. *J. Incl. Phenom.* **1988**, *6*, 167–174.
9. Badawy, S.I.F.; Ghorab, M.M.; Adeyeye, C.M. Characterization and bioavailability of danazol-hydroxypropyl  $\beta$ -cyclodextrin coprecipitates. *Int. J. Pharm.* **1996**, *128*, 45–54.
10. Hersey, A.; Robinson, B.H. Thermodynamic and kinetic study of the binding of azo-dyes to  $\alpha$ -cyclodextrin. *J. Chem. Soc. Faraday Trans. 1* **1984**, *80*, 2039–2052.
11. Frömming, K.H.; Szejtli, J. *Cyclodextrins in Pharmacy*; Kluwer Academic Publishers: The Netherlands, 1994.
12. Higuchi, T.; Connors, K.A. Phase-solubility techniques. *Adv. Anal. Chem. Instru.* **1965**, *4*, 117–212.
13. VanEtten, R.L.; Sebastian, J.F.; Clowes, G.A.; Bender, M.L. Acceleration of phenyl cleavage by cycloamyloses. A model of enzymatic specificity. *J. Am. Chem. Soc.* **1967**, *89*, 3242–3252.



14. Martin, A. *Physical Pharmacy, Physical Chemical Principles in the Pharmaceutical Sciences*, 4th Ed.; Lea and Febiger: Philadelphia, 1993.
15. Simonelli, A.P.; Mehta, S.C.; Higuchi, W.I. Dissolution rates of high energy sulfathiazole povidone coprecipitate II. Characterization of form of drug controlling its dissolution rate via solubility studies. *J. Pharm. Sci.* **1976**, *65*, 355–361.
16. Chan, K.L.; Yuen, K.H.; Sunil, J.; Peh, K.K.; Toh, W.T. A high-performance liquid chromatography analysis of plasma artemisinin using a glassy carbon electrode for reductive electrochemical detection. *Planta. Med.* **1997**, *63*, 66–69.
17. Loftsson, T.; Brewster, M.E. Pharmaceutical applications of cyclodextrins. Drug solubilization and stabilisation. *J. Pharm. Sci.* **1996**, *85* (10), 1017–1025.
18. Duchêne, D. *Cyclodextrins and Their Industrial Uses*; Editions de Santé: Paris, 1987.
19. Harrison, J.C.; Eftink, M.R. Cyclodextrin-adamantanecarboxylate inclusion complexes: a model system for the hydrophobic effect. *Biopolymers* **1982**, *21*, 1153–1166.
20. Bergeron, R.J. Cycloamylose-substrate binding. In: *Inclusion Compound Vol. 3. Physical Properties and Applications*; Atwood, J.L., Davies, J.E.D., MacNicol, D.D., Eds.; Academic Press: London, 1984.
21. Cromwell, W.C.; Byström, K.; Eftink, M.R. Cyclodextrin-adamantanecarboxylate inclusion complexes: studies of the variation of cavity size. *J. Phys. Chem.* **1985**, *89*, 326–332.



Copyright of Drug Development & Industrial Pharmacy is the property of Taylor & Francis Ltd and its content may not be copied or emailed to multiple sites or posted to a listserv without the copyright holder's express written permission. However, users may print, download, or email articles for individual use.